Electrical manipulation of the fine-structure splitting of WSe_2 quantum emitters

Electrical manipulation of the fine-structure splitting of WSe_2 quantum emitters

Chitraleema Chakraborty
Materials Science, University of Rochester, Rochester, New York 14627, USA;
Electrical Engineering and Computer Science, Massachusetts Institute of Technology, Cambridge, Massachusetts 02139, USA;
and John A. Paulson School of Engineering and Applied Sciences, Harvard University, Cambridge, Massachusetts 02138, USA

Nicholas R. Jungwirth
School of Applied and Engineering Physics, Cornell University, Ithaca, New York 14850, USA

Gregory D. Fuchs
School of Applied and Engineering Physics, Cornell University, Ithaca, New York 14850, USA
and Kavli Institute at Cornell for Nanoscale Science, Ithaca, New York 14853, USA

A. Nick Vamivakas*
Materials Science, University of Rochester, Rochester, New York 14627, USA;
Center for Coherence and Quantum Optics, University of Rochester, Rochester, New York 14627, USA;
Institute of Optics, University of Rochester, Rochester, New York 14627, USA;
and Department of Physics and Astronomy, University of Rochester, Rochester, New York 14627, USA

(Received 21 June 2018; published 24 January 2019)

We report on the modulation of the fine-structure splitting of quantum-confined excitons in localized quantum emitters hosted by a monolayer transition metal dichalcogenide (TMDC). The monolayer TMDC, tungsten diselenide (WSe_2), is encapsulated in a van der Waals heterostructure which enables the application of an external electric field on the quantum-dot-like emitters hosted by the monolayer flake. The emitters exhibit quantum-confined Stark effect and a modulation in the fine-structure splitting (FSS) as a function of electric field. A maximum modulation of 1500 μeV is observed in the FSS from the studied emitters. Finally, we measure the polarization response of the localized exciton emission as a function of electric field exhibiting strong circular polarization with decreasing fine-structure splitting, further confirming the suppression of the anisotropic electron-hole exchange interaction thats causes the FSS.

DOI: 10.1103/PhysRevB.99.045308

I. INTRODUCTION

Semiconducting quantum dots (QDs) are among the most promising sources of nonclassical light because they can generate on-demand single photons for applications in quantum key cryptography and quantum optics [1]. Ideally, QDs could also provide pairs of indistinguishable entangled photons on demand, which are valuable for quantum networking [2]. One approach is to take advantage of the biexciton to exciton radiative cascade [3]. However, this has been problematic due to the presence of a fine-structure splitting [4,5] in the QD emission which limits the indistinguishability of the entangled photon pairs.

Fine-structure splitting can originate, for example, from a decrease in the symmetry for the quantum dots leads to the mixing of their excitonic spin states due to the anisotropic electron-hole exchange interaction. Further, this leads to an energetic splitting in the emission of the neutral exciton. The magnitude of the FSS depends on the shape, anisotropic strain, composition, and the crystal inversion symmetry [3]. For the generation of entangled photon pairs, the FSS needs to be eliminated. External perturbations such as strain, electric field, and magnetic field, or sometimes a combination of different knobs are used to erase the FSS in epitaxially grown quantum dots [6,7].

Recently, optically active quantum-dot-like emitters were discovered in several two-dimensional (2D) materials such as transition metal dichalcogenides (TMDCs) [8–11], hexagonal boron nitride (hBN) [12], and GaSe [13]. Their origins have been attributed to defects [12], naturally occurring imperfections in exfoliated [8–10,14,15] or chemical vapor deposition (CVD) [11] grown monolayer flakes. Furthermore, they can also be deterministically created by engineering the strain profile of these layered materials [16–19]. The 2D host of the quantum emitters offers easy integration with current devices in optoelectronics or quantum technologies. Moreover, 2D layers offer more tunability than conventional 3D hosts due to the possibility of making devices based on van der Waals heterostructures [20–23]. Similar to the epitaxially grown quantum dots, a FSS at zero magnetic field due to an anisotropic electron-hole exchange interaction in the TMDC quantum dots has been also observed [8,9,11,16,23,24]. A zero-field splitting of up to 800 μeV [8,9,11,16] has been

*nick.vamivakas@rochester.edu

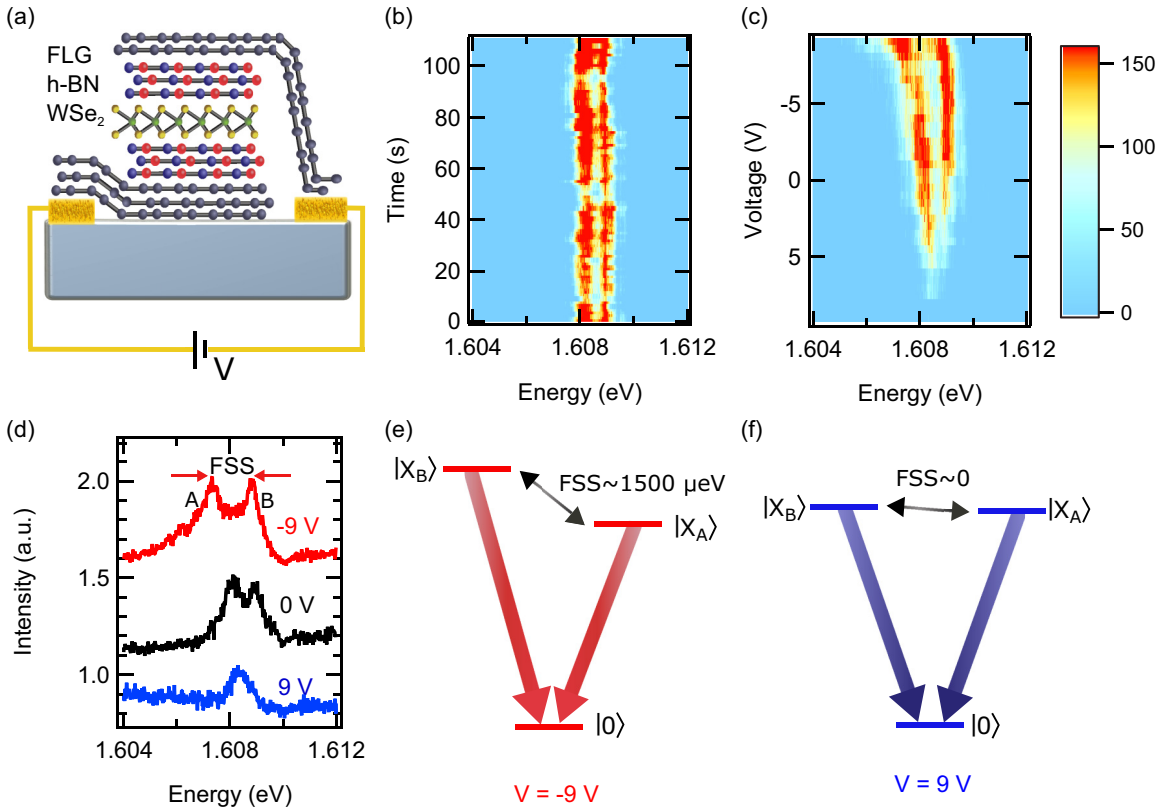

FIG. 1. (a) Device schematic showing the van der Waals assembly on a substrate with prepatterned electrodes. (b) Time trace of the photoluminescence (PL) spectra from the studied doublet peak exhibiting correlated spectral wandering. (c) PL as a function of applied voltage (V) showing modulation of the FSS. (d) Spectral linecut at three different voltages. Energy level diagram at (e) $V = -9$ V and (f) $V = 9$ V showing maximum and minimum FSS at the two different applied voltages.

recorded, which is almost an order of magnitude larger than InAs quantum dots, a feature attributed to the strong Coulomb interactions in TMDCs [16]. In this paper, we will demonstrate the control of the fine-structure splitting of the excitons in these quantum-dot-like emitters by applying a vertical electric field.

II. DEVICE GEOMETRY AND EXPERIMENTAL SETUP

The device used in this experiment is a van der Waal's heterostructure hosting optically active QDs in monolayer tungsten diselenide (WSe_2). A schematic of the device is presented in Fig. 1(a). The device has a capacitorlike geometry with few-layer graphene (FLG) serving as the top and bottom electrodes that is connected to an external Keithley 2400 sourcemeter for applying voltage (V). Few-layer hexagonal boron nitride (hBN) ($\sim$15 nm) is used as the dielectric material on either side of the monolayer WSe_2 which hosts the quantum emitters. This geometry enables the application of a vertical electric field which is sensed by the emitters in WSe_2. Such a van der Waals heterostructure integrated with TMDC quantum emitters has previously demonstrated a strong quantum-confined Stark effect [22], efficient electroluminescence [20,21], and controlled generation of charged excitons in TMDC QDs [23]. We perform the optical measurements in an Attodry cryostat with an 1.837 eV excitation laser focused with an objective having a numerical aperture of 0.82.

III. VOLTAGE CONTROLLED FINE-STRUCTURE SPLITTING

Figure 1(b) presents the photoluminescence (PL) spectral map as a function of time. From the color plot in Fig. 1(b), we see two split peaks owing to the fine-structure splitting. The two peaks also exhibit correlated spectral wandering due to random fluctuations in the local environment of the quantum dot. This suggests that both peaks originate from the same confined exciton. We refer to these two split peaks from the same QD as a doublet. The energy splitting between the two peaks of the doublet results in a value of $\sim$800 μeV for the FSS at zero voltage. This is consistent with the splitting observed in previous reports [8,9,11].

Next, we study the correlation between the FSS and the applied voltage (V). Figure 1(c) presents the voltage-dependent PL map of the doublet showing a modulation of the emission energy due to the quantum-confined Stark effect (QCSE) of the emitters [22]. This is also clear in the spectral linecuts from three different voltage points plotted in Fig. 1(d). From Figs. 1(c) and 1(d), we can see that the energy splitting between the doublet (FSS) is also modulated along with a shift in their individual emission energies. This is illustrated by the energy level diagram in Figs. 1(e) and 1(f). At $V = -9$ V, we observe the maximum splitting of $\sim$1500 μeV. On sweeping the voltage to the positive direction the FSS reduces and shows a minimum at $V = 9$ V. QCSE is also accompanied by a

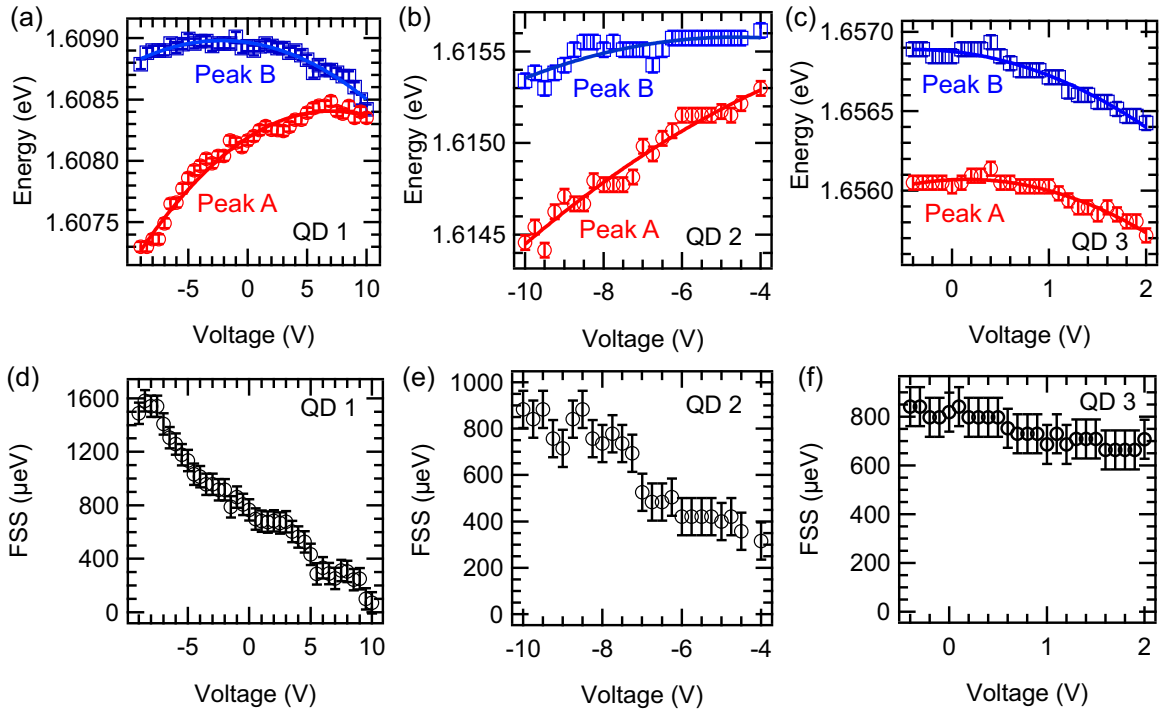

FIG. 2. (a)–(c) Extracted peak energies of the doublet from three QDs as a function of voltage. Solid lines are fit to Stark shift equation (1). (d)–(f) FSS as a function of applied voltage for the three QDs. Error bars represent the spectral resolution of the setup.

reduction in intensity and broadening of the linewidth due to the onset of the nonradiative tunneling effect [22]. Thus, at $V > 9$ V, the PL intensity is significantly reduced and the peak is broadened, which makes it difficult to resolve the FSS.

In Figs. 2(a)–2(c), we plot the extracted peak position obtained from three different QDs. The PL emission energies from the two lines of the doublets are fit to

$$E = E_0 - \mu F - \tfrac{1}{2}\alpha F^2, \tag{1}$$

where E_0 is the zero-field transition energy, F is the local electric field acting at the emitter, and μ and α are the dipole moment and polarizability, respectively, between the ground and excited states. F is calculated from the applied voltage (V) by the Lorentz local field approximation [25], $F = V(\epsilon + 2)/(3t)$, where ϵ is the dielectric constant and t is the thickness of the surrounding hBN environment. Our device is approximately 30 nm thick, and the dielectric constant of hBN [26] is taken to be 3. It is well known that the Coulomb exchange interaction can be modified by the Stark effect because the electric field can modify the overlap of the carrier wave functions [27]. In this case, we see that both eigenstates of the excitons shift at different rates as a function of the applied electric field for the three QD doublets presented in Figs. 2(a)–2(c). The orientation of the dipole with respect to the electric field could affect the two states unequally along the electric field direction [3]. This leads to a nearly monotonic change in the FSS [Figs. 2(d)–2(f)] observed up to the resolution limit of our setup (0.02 nm or 40 μeV).

The maximum Stark shift and the fitting parameters for the quantum emitters are summarized in Table I. From the table, QD1 exhibits a maximum change in the FSS accompanied by a maximum average Stark shift ($\Delta E^{a,b}_{\text{avg}}$) of 750 μeV. QD2 and QD3 exhibit a relatively low ΔFSS which can be correlated with the reduced shift in the average peak emission energies than QD1. Further, the magnitude and sign of the dipole moment of the two peaks of the doublet are different for all the three emitters which allows the peaks to converge as a function of applied voltage. Thus, we see that the emitter's dipole orientation with respect to the electric field strongly affects the fine-structure splitting. Due to this, two different external perturbations are used in earlier experiments (combination of strain and electric field) [28], where one perturbation is used to align the orientation of the exciton along the axis of the other control knob for complete reduction of the fine-structure splitting of the doublet emission state.

In the case of epitaxially grown QDs, strain has been used to align the QD exciton along a preferred direction of the

TABLE I. Correlation of the Stark effect with the modulation of the FSS. ΔFSS and ΔE are the maximum change in FSS and emission energy in μeV, respectively. $\Delta E^{a,b}_{\text{avg}}$ is the average Stark shift (ΔE) of the two peaks of the doublet.

QD	ΔFSS	Peak	ΔE	$\Delta E^{a,b}_{\text{avg}}$	μ (D)	α (Å)
QD1	1490	Peak A	1100	750	−0.059	5.2
		Peak B	400		0.013	3.6
QD2	567	Peak A	800	550	−0.044	7.7
		Peak B	300		0.07	9.1
QD3	150	Peak A	400	450	−0.008	97.8
		Peak B	500		0.069	95.6

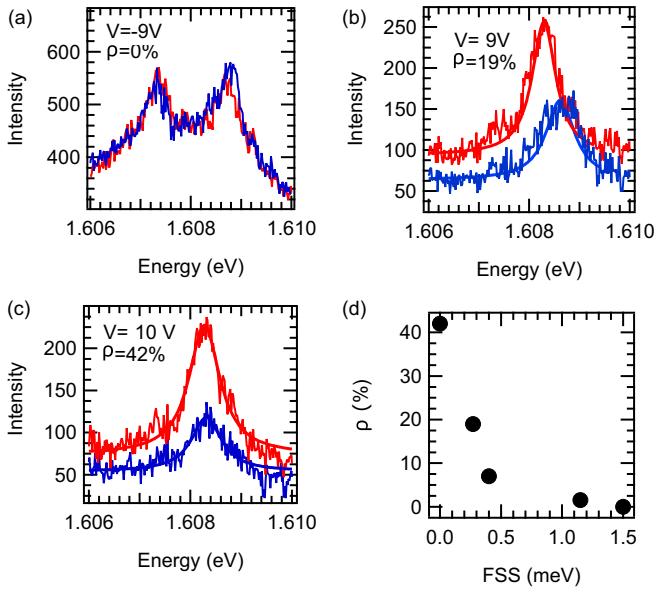

FIG. 3. Circular polarization resolved PL spectra at different voltages: (a) −9 V, (b) 9 V, and (c) 10 V. The red (blue) curve is σ^+ (σ^-) polarized photoluminescence emission. Solid lines are Lorentzian fits. (d) Degree of circular polarization (ρ) as a function of fine-structure splitting.

electric field where the electric field effect is maximized. Both the strain and electric field act as an effective deformation to restore the symmetry of the quantum dots. The emitters embedded in monolayer WSe_2 can be under the influence of random strain fields due to imperfections in the exfoliated crystal which may or may not align the emitter along the electric field. This is why we see a modulation in the FSS only in 10%–15% of the emitters studied in the different heterostructure devices which also vary from emitter to emitter. Further, our findings suggests that the electric field (F) is highly dependent on the position of the emitter and its local environment which leads to different behavior for the different observed emitters.

IV. CIRCULAR POLARIZATION RESOLVED PHOTOLUMINESCENCE

Because the finite spectral resolution of the experimental setup does not let us prove FSS = 0, we measure the circular polarization of the exciton peaks. For the case of the quantum dots, the degeneracy in the exciton state is lifted due to asymmetric confinement, for example, by strain, which leads to linearly polarized eigenstates [8,11]. A complete reduction in the degeneracy restores the circular polarization of the exciton state given by the spin-valley coupling. The degree of circular polarization is defined as

$$\rho = \frac{I_{\sigma^+} - I_{\sigma^-}}{I_{\sigma^+} + I_{\sigma^-}} \times 100\%, \qquad (2)$$

where I_{σ^+} and I_{σ^-} are intensities for σ^+ and σ^- detection. Circular polarization resolved PL spectra at different input voltages are shown in Fig. 3. The degree of circular polarization is expected to increase as the fine-structure approaches zero [29]. In this case the exciton is no longer a mixture of the spin-valley states as the FSS approaches zero. In Fig. 3(a), the PL lines are unpolarized in the circular basis. Increasing the voltage in the positive direction leads to an enhancement in the degree of circular polarization of up to 42% [Fig. 3(c)]. Although this indicates that a FSS is still present, it could not be detected any further due to the resolution limit of the setup. The spectral resolution can be improved by using a Fabry-Pérot interferometer which is the direction of a future study. On increasing the voltage beyond 10 V, the device switches to the tunneling regime for this QD where the confinement energies have been reduced to the extent that the electron-hole pairs tunnel out from the emitter. Therefore, we are limited by the confinement energies which limit us from applying a higher field which could potentially restore the symmetry of the emitter to provide unity degree of circular polarization. To overcome this, emitters with a deeper confinement potential could be designed by engineering the strain in the device or an additional strain control knob can be used along with an electric field.

V. CONCLUSION

In summary, we have demonstrated the manipulation of the FSS by applying an external voltage. This has been further confirmed by the enhancement in the degree of circular polarization due to reduced mixing from the electron-hole Coulomb exchange interactions. Such electric field devices are well suited to be integrated to low volume cavities enabling higher efficiencies of optical coupling and cavity QED effects with large Purcell enhancements [30,31]. In the future, a field-effect device with deterministically created quantum dots fabricated on a piezoelectric or flexible substrate can be employed to apply a combination of strain and electric field to observe a more versatile and effective modulation of the FSS. This work identifies a clear path to fully suppressing FSS, which enables the cascaded biexciton emission [32] to be used as a source of entangled photons in scalable solid-state-based quantum information technology.

ACKNOWLEDGMENTS

This work was supported by NSF EFRI EFMA-1542707, NSF CAREER DMR 1553788, AFOSR FA9550-16-1-0020, the Cornell Center for Materials Research—an NSF MRSEC (DMR 1719875), and the Leonard Mandel Faculty Fellowship in Quantum Optics.

[1] A. J. Shields, Nat. Photonics **1**, 215 (2007).
[2] H. J. Kimble, Nature (London) **453**, 1023 (2008).
[3] A. J. Bennett, M. A. Pooley, R. M. Stevenson, M. B. Ward, R. B. Patel, A. B. de la Giroday, N. Sköld, I. Farrer, C. A. Nicoll, D. A. Ritchie, and A. J. Shields, Nat. Phys. **6**, 947 (2010).
[4] M. Bayer, A. Kuther, A. Forchel, A. Gorbunov, V. B. Timofeev, F. Schäfer, J. P. Reithmaier, T. L. Reinecke, and S. N. Walck, Phys. Rev. Lett. **82**, 1748 (1999).
[5] M. Bayer, G. Ortner, O. Stern, A. Kuther, A. A. Gorbunov, A. Forchel, P. Hawrylak, S. Fafard, K. Hinzer, T. L. Reinecke,

S. N. Walck, J. P. Reithmaier, F. Klopf, and F. Schäfer, Phys. Rev. B **65**, 195315 (2002).

[6] S. Kumar, E. Zallo, Y. H. Liao, P. Y. Lin, R. Trotta, P. Atkinson, J. D. Plumhof, F. Ding, B. D. Gerardot, S. J. Cheng, A. Rastelli, and O. G. Schmidt, Phys. Rev. B **89**, 115309 (2014).

[7] R. Trotta, P. Atkinson, J. D. Plumhof, E. Zallo, R. O. Rezaev, S. Kumar, S. Baunack, J. R. Schröter, A. Rastelli, and O. G. Schmidt, Adv. Mater. **24**, 2668 (2012).

[8] A. Srivastava, M. Sidler, A. V. Allain, D. S. Lembke, A. Kis, and A. Imamoğlu, Nat. Nanotechnol. **10**, 491 (2015).

[9] C. Chakraborty, L. Kinnischtzke, K. M. Goodfellow, R. Beams, and A. N. Vamivakas, Nat. Nanotechnol. **10**, 507 (2015).

[10] P. Tonndorf, R. Schmidt, R. Schneider, J. Kern, M. Buscema, G. A. Steele, A. Castellanos-Gomez, H. S. J. van der Zant, S. Michaelis de Vasconcellos, and R. Bratschitsch, Optica **2**, 347 (2015).

[11] Y.-M. He, G. Clark, J. R. Schaibley, Y. He, M.-C. Chen, Y.-J. Wei, X. Ding, Q. Zhang, W. Yao, X. Xu, C.-Y. Lu, and J.-W. Pan, Nat. Nanotechnol. **10**, 497 (2015).

[12] T. T. Tran, K. Bray, M. J. Ford, M. Toth, and I. Aharonovich, Nat. Nanotechnol. **11**, 37 (2016).

[13] P. Tonndorf, S. Schwarz, J. Kern, I. Niehues, O. Del Pozo-Zamudio, A. I. Dmitriev, A. P. Bakhtinov, D. N. Borisenko, N. N. Kolesnikov, A. I. Tartakovskii, S. Michaelis de Vasconcellos, and R. Bratschitsch, 2D Mater. **4**, 021010 (2017).

[14] C. Chakraborty, K. M. Goodfellow, and A. N. Vamivakas, Opt. Mater. Exp. **6**, 2081 (2016).

[15] A. Branny, G. Wang, S. Kumar, C. Robert, B. Lassagne, X. Marie, B. D. Gerardot, and B. Urbaszek, Appl. Phys. Lett. **108**, 142101 (2016).

[16] S. Kumar, A. Kaczmarczyk, and B. D. Gerardot, Nano Lett. **15**, 7567 (2015).

[17] C. Palacios-Berraquero, D. M. Kara, A. R.-P. Montblanch, M. Barbone, P. Latawiec, D. Yoon, A. K. Ott, M. Loncar, A. C. Ferrari, and M. Atatüre, Nat. Commun. **8**, 15093 (2017).

[18] A. Branny, S. Kumar, R. Proux, and B. D. Gerardot, Nat. Commun. **8**, 15053 (2017).

[19] N. V. Proscia, Z. Shotan, H. Jayakumar, P. Reddy, C. Cohen, M. Dollar, A. Alkauskas, M. Doherty, C. A. Meriles, and V. M. Menon, Optica **5**, 1128 (2018).

[20] C. Palacios-Berraquero, M. Barbone, D. M. Kara, X. Chen, I. Goykhman, D. Yoon, A. K. Ott, J. Beitner, K. Watanabe, T. Taniguchi, A. C. Ferrari, and M. Atatüre, Nat. Commun. **7**, 12978 (2016).

[21] G. Clark, J. R. Schaibley, J. Ross, T. Taniguchi, K. Watanabe, J. R. Hendrickson, S. Mou, W. Yao, and X. Xu, Nano Lett. **16**, 3944 (2016).

[22] C. Chakraborty, K. M. Goodfellow, S. Dhara, A. Yoshimura, V. Meunier, and A. N. Vamivakas, Nano Lett. **17**, 2253 (2017).

[23] C. Chakraborty, L. Qiu, K. Konthasinghe, A. Mukherjee, S. Dhara, and A. N. Vamivakas, Nano Lett. **18**, 2859 (2018).

[24] S. Kumar, M. Brotóns-Gisbert, R. Al-Khuzheyri, G. Ballesteros-Garcia, J. F. Sánchez-Royo, and B. D. Gerardot, Optica **3**, 882 (2016).

[25] P. Tamarat, T. Gaebel, J. R. Rabeau, M. Khan, A. D. Greentree, H. Wilson, L. C. L. Hollenberg, S. Prawer, P. Hemmer, F. Jelezko, and J. Wrachtrup, Phys. Rev. Lett. **97**, 083002 (2006).

[26] K. K. Kim, A. Hsu, X. Jia, S. M. Kim, Y. Shi, M. Dresselhaus, T. Palacios, and J. Kong, ACS Nano **6**, 8583 (2012).

[27] M. Z. Maialle, E. A. de Andrada e Silva, and L. J. Sham, Phys. Rev. B **47**, 15776 (1993).

[28] R. Trotta, E. Zallo, C. Ortix, P. Atkinson, J. D. Plumhof, J. van den Brink, A. Rastelli, and O. G. Schmidt, Phys. Rev. Lett. **109**, 147401 (2012).

[29] M. Ghali, Y. Ohno, and H. Ohno, Appl. Phys. Lett. **107**, 123102 (2015).

[30] A. K. Nowak, S. L. Portalupi, V. Giesz, O. Gazzano, C. D. Savio, P.-F. Braun, K. Karrai, C. Arnold, L. Lanco, I. Sagnes, A. Lemaître, and P. Senellart, Nat. Commun. **5**, 3240 (2014).

[31] C. Böckler, S. Reitzenstein, C. Kistner, R. Debusmann, A. Löffler, T. Kida, S. Höfling, A. Forchel, L. Grenouillet, J. Claudon, and J. M. Gérard, Appl. Phys. Lett. **92**, 091107 (2008).

[32] Y.-M. He, O. Iff, N. Lundt, V. Baumann, M. Davanco, K. Srinivasan, S. Höfling, and C. Schneider, Nat. Commun. **7**, 13409 (2016).